American Scientific Research Journal for Engineering, Technology, and Sciences (ASRJETS)
ISSN (Print) 2313-4410, ISSN (Online) 2313-4402

http://asrjetsjournal.org/

Image De-noising using 2-D Circular-Support Wavelet Transform

Adil Aydiki[a*], Omar Y. Ismael[b], Fatih Başçiftçi[c]

[a]*Selcuk University, Konya 42030, Turkey*
[b]*Ninevah University, Mosul 41001, Iraq*
[c]*Selcuk University, Konya 42030, Turkey*
[a]*Email: adil.shingary86@hotmail.com*
[b]*Email: omar.ismael@uoninevah.edu.iq*
[c]*Email: basciftci@selcuk.edu.tr*

Abstract

Images are often suffering from two main corruptions (unwanted modifications). These modifications in image accuracy are categorized as blur and noise. Noise appears during different image processing phases of acquisition, transmission, and retrieval. The purpose of any de-noising algorithm is to remove such noise while maintaining as much as possible image details. A 2-D circular-support wavelet transform (2-D CSWT) is anticipated in this paper to be utilized as an image de-noising algorithm. The realization of such de-noising algorithm is accomplished in the form of some competent mask filters. De-noising by thresholding processes can be applied on all 2-D high-pass coefficient channels with different thresholding levels. Lena noisy image with different levels of noise (Salt and Pepper, and Gaussian) has been used to assess the performance of such de-noising scheme. Test are done in terms of PSNR and correlation factor of the reconstructed image. A comparative study between the Conventional wavelet transform and the 2-D CSWT done in this paper.

Keywords: Gaussian noise; Salt and pepper noise; Conventional wavelet transform; Circular wavelet transform; 2-D circular decomposition; 2-D circular reconstruction; De-noising by thresholding; Correlation factor; PSNR.

---

* Corresponding author.

1. Introduction

In classical terms, 2-D wavelet transform is an extension of the 1-D wavelet transform of Figure 1 To obtain a 2-D transform, the 1-D transform is first applied across all the rows and then across all the columns at each decomposition level.

Four sets of coefficients are generated at each decomposition level: LL as the average, LH as the details across the horizontal direction, HL as the details across the vertical direction and HH as the details across the diagonal direction.

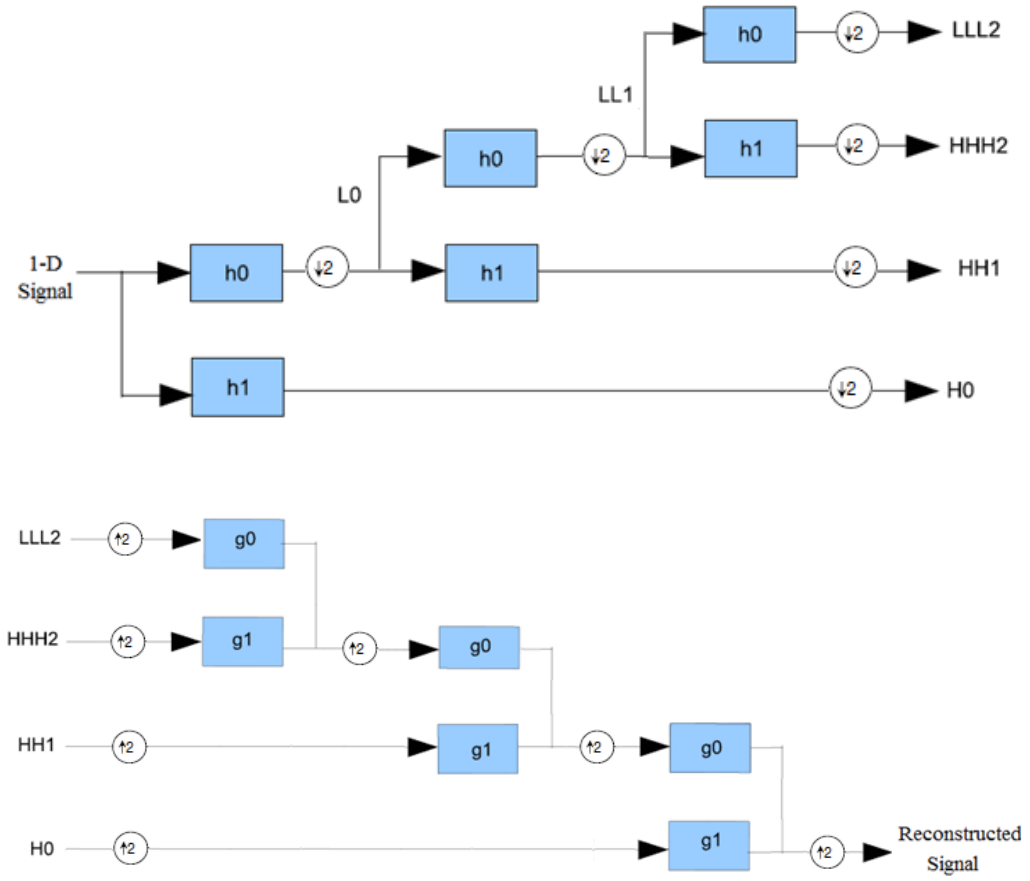

Figure 1: 1-D 3-level wavelet transform and it's inverse.

In 2-D case, the original image signal $x(m, n)$ can be considered as if it is a combination of 1-D row signals and 1-D column signals. In 2-D Discrete Wavelet Transform (DWT), each row of the image is processed first, then each column is processed as it is done in 1-D case. Figure 2 demonstrates a one-level image decomposition and reconstruction. In a similar way as in signal decomposition, the subsampling process is applied after each filtering. The whole process results in four sub-images, namely; approximation component and horizontal, vertical & diagonal details. The resulting sub-images have quarter the size of the original image, that because of the sub-sampling after each filtering.

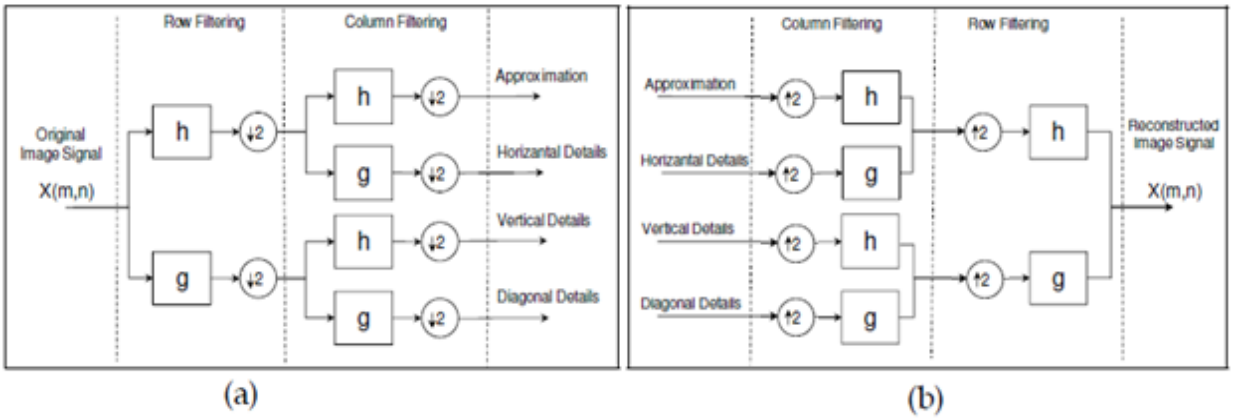

Figure 2: One-level DWT steps of a 2-D image. (a) Decomposition, (b) Reconstruction.

A classical wavelet de-noising scheme is shown in Figure 3, it consists of 2-D wavelet transform, 2-D inverse wavelet transform and an intermediate thresholding stage to shrink wavelet coefficients. In such thresholding stage, the level of the noise is first estimated and the appropriate thresholds are set. It should be noted that an important point in thresholding is to set a suitable value for the threshold level. Recently, many approaches have been given for calculating the threshold value. Most of those approaches require the noise level estimation. However, a useful tool for an estimator is the standard deviation of the data values. A good estimator σ for the wavelet de-noising is proposed by Donoho [1] and given as;

$$\sigma = \frac{median(d_{L-1,k})}{0.6745}, \quad k = 0,1,\ldots,2^{L-1}-1$$

where L denotes the number of decomposition levels. The median selection is applied on the detail coefficient of the decomposed signal.

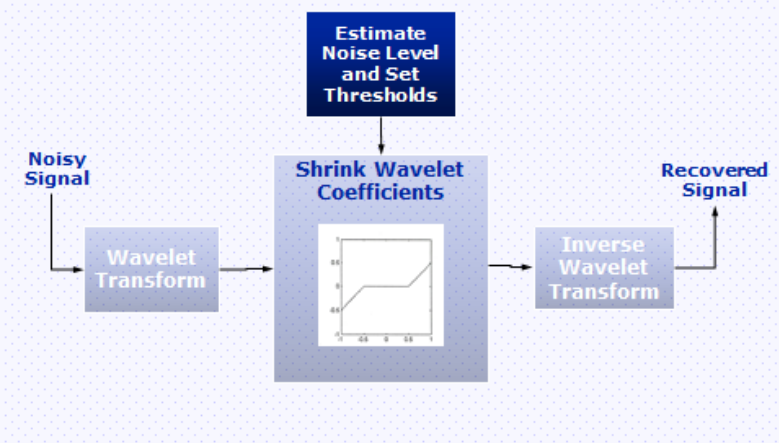

Figure 3: A classical scheme for wavelet de-noising

In Figure 3, the intermediate stage of wavelet coefficient shrinking (*i. e.*, thresholding) can be performed either

by hard thresholding or by soft thresholding strategies (as shown in Figure 4). Generally, thresholding process will allow the detail coefficients which are greater than the threshold level to pass (*i. e.*, considering them as image high frequency components) while preventing the lower level coefficients from passing through the threshold (*i. e.*, considering them as noise components). There are many property considerations and limitation of the two strategies of thresholding. The hard thresholding strategy is usually unstable and very sensitive to the small changes in pixel level. On other side, the soft thresholding strategy may result in unnecessary bias level for true large coefficients. To overcome the drawbacks of the described nonlinear strategies of thresholding, many sophisticated methods are proposed. Despite that, hard and soft thresholding are still applicable and treated as the most reliable and efficient thresholding techniques.

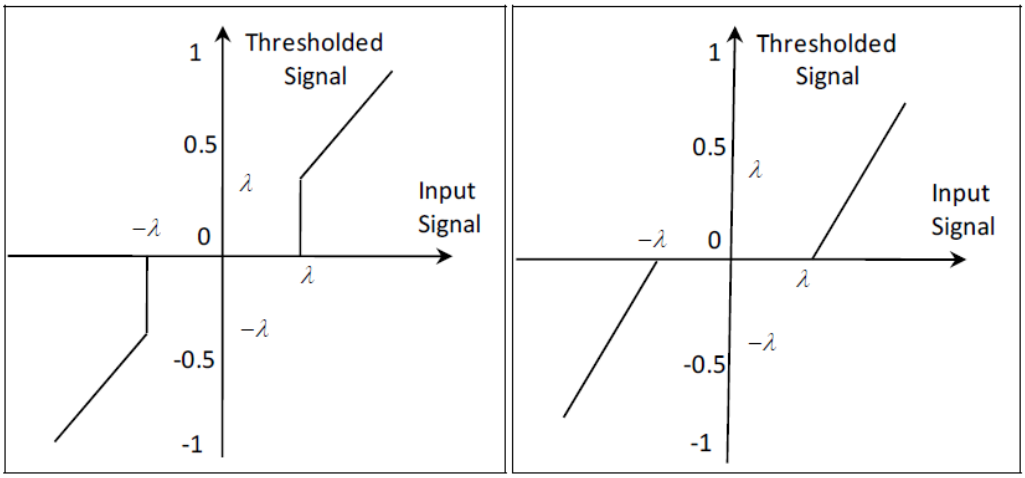

(a) Hard thresholding,

(b) Soft thresholding.

Figure 4: Thresholding strategies.

2. Literature Review

Many attempts were accomplished to de-noising noisy images, resulting in a wide variation in the output de-noised image performances.

In 2007, architectures for 1-D and 2-D discrete wavelet transform (DWT) using lifting schemes were presented [2]. An embedded decimation technique was exploited to optimize the architecture for 1-D DWT, which was designed to receive an input and generate an output with the low- and high-frequency components of original data being available alternately. An efficient line-based architecture for 2-D DWT was extended based on the 1-D DWT lifting scheme architecture by employing parallel and pipeline techniques. Such techniques were mainly composed of two horizontal filter modules and one vertical filter module, working in parallel and pipeline fashion with 100% hardware utilization. Two 2-D fast architectures were presented. They can perform J levels of decomposition for (N * N -sized) image in approximately 2N2(1 - 4(-J))/3 internal clock cycles. Compared

with some other works reported in previous literature, the lifting scheme architectures for 2-D DWT were proved to be efficient alternatives in tradeoff among hardware cost, throughput rate, output latency and control complexity.

In many other wavelet-based techniques, it has been proved that these techniques can offer good processing quality and best flexibility for the problem of noise in both 1-D signals & 2-D images. Noise-existence in image processing and applications is practically one of the most important problems to solve because it affects the overall performance of the imaginary systems. Therefore, various methods were developed by Turkish authors for de-noising. In 2007, M. İkiz and his colleagues [3], presented a comparison of some wavelet de-noising methods with some recent methods, highlighting some of wave transform properties. Also in 2007, M. İkiz and his colleagues [4], suggested a classification system used to recognize the speaker identity by means of wavelet analysis and neural network approach. After sampling, the 1-D voice signals generated from 10 different persons (6 males and 4 females) were de-noised using Wave-flow and Wave-pad shareware programs. A Matlab Simulink model was designed to generate the tested data from the voice signals. This data was applied once again as an input signal for a Matlab-based neural network to classify the voice data into different speakers. Again in 2007, B. Demir and S. Ertürk [5] proposed a hyperspectral image classification approach using support vector machines (SVM) after a wavelet de-noising. The noise reduction was carried out in each band independently. Compared with direct SVM based classification, it was shown that the SVM classification of de-noised images can result in significantly better classification accuracy, improved sparsity and faster testing time. Such properties make the wavelet de-noised SVM based hyperspectral classification approach more suitable for low-complex and real-time applications.

In 2010, a de-noising algorithm based on the Haar wavelet transform was presented. The methodology was based on an algorithm initially developed for image compression using the Tetrolet transform. The Tetrolet transform is basically an adaptive Haar wavelet transform whose support is tetrominoes, that is, shapes made by connecting four equal sized squares. That algorithm gave 2.5 dB improvement in peak signal-to-noise ratio (PSNR) over the classical Haar wavelet transform for some de-noised test images corrupted previously by an additive white Gaussian noise (AWGN) with the assumption of universal hard thresholding. By such algorithm, it had been shown that the algorithm was local and can work independently on each 4x4 block of the image. In addition, the algorithm was well suited for efficient hardware implementation because of its local nature and the simplicity of its computations [6].

In 2011, B. Ergen and M. Baykara [7] gave a comparison between the wavelet and wavelet package decomposition for image de-noising. They examined many standard test images and their results showed that increasing of decomposition depth has no effect on improving the values of peak signal- to-noise ratio (PSNR). They concluded that wavelet decomposition is superior to wavelet package decomposition and more suitable to be used in image de-noising. In addition, the performances of wavelet de-noising methods were examined in 2012 by B. Ergen [1] for several variations including various rules of thresholding with different types of wavelet filters. Comparisons were accomplished for the three estimation methods of threshold with different wavelet types. Results have shown that the decomposition level is the most important controlling factor in wavelet de-noising, rather than the wavelet type. It has been shown that neither the threshold type nor the

estimation of threshold value has any effect on the de-noising quality.

However, no worthy differences in the resulting de-noised images were seen till the 6-level decomposition, after such level, a better performance in terms of SNR level for Rigresure method was achieved over the others. Also, it was shown that the wavelet type was not very important for large oscillation numbers and the decomposition level was absolutely dependent on the frequency band of the image to be analyzed and its sampling frequency. Radar constitutes one of the major application areas of communication systems.

While radar signal passes from source to target, the noise may be mixed with the original signal because of environmental or human-induced reasons. Thus, because of that noise, it may be impossible to read the radar signal correctly. In 2014, M. Üstündağ and his colleagues.

Reference [8] suggested a non-traditional wavelet packet transform (WPT) for the de-noising of weak radar signals with high-performance. While such non-traditional WPT transform were performed, the appropriate wavelet family type, entropy type and decomposition level number were instantaneously selected by applying the genetic algorithm (GA) structure as an intelligent system for optimization. Moreover, the suitable threshold function was selected using the fuzzy s-function as a thresholding function and variable parameters of this function were set according to the best performance criteria. The method was then compared with other algorithms available in the literature for de-noising of the weak radar signals. The system performance was tested using root mean square error and the correlation coefficient criteria as metrics. Results highlighted that the suggested method gave better performance evaluations than the other de-noising methods available in the literature. Recently, in 2015, A. Srivastava and S. Maheshwari [9] presented a work that reviewed and summarized the use of wavelet transform for de-noising of signals contaminated with noise. Their work also discussed the diverse applications of the wavelet transform. In the paper, in 2015, a quantum Boolean image processing methodology was presented by M. Mastriani [10] with special emphasis in image de-noising. An approach for internal image representation was presented, highlighting two new interfaces: classical-to-quantum and quantum-to-classical. That image de-noising was called quantum Boolean mean filter and worked exclusively with computational basis states (CBS). In that sense, the image was decomposed into its three color components (red, green and blue). Then, the bit-planes were obtained for each color (with 8 bits per pixel), i.e., 8 bit-planes per color. All operations were accomplished using the most significant bit (MSB) bit-plane of each color, exclusive manner. After a classical-to-quantum interface (which included a classical inverter), a quantum Boolean version of the image was achieved within the quantum machine. The methodology prevented the problem of quantum measurement, which alters the results of the measured except in the case of CBS. Inside quantum machine, the results of filtering the inverted version of MSB, were passed through a quantum-to-classical interface (which involves another classical inverter) by proceeding to reassemble each color component. Finally, this processing methodology was concluded by filtering the image and discussing some appropriate metrics for image de-noising in a set of experimental results.

Such metrics include the correlation factor and Peak signal-to-noise ratio (PSNR). It had been shown that the results of such quantum Boolean de-noising methodology were superior to those obtained by the classical techniques.

3. 2-D Circular-Support Wavelet Transform for Image De-noising

in 2013, a geometrical image transform called 2-D CSWT was presented [11] based on the theory of the 2-D elliptical–support wavelet filter bank [12]. The circularly-decomposed frequency subspaces (2-D circular spectral split schemes) can efficiently represent images [13]. The designed 2-D circular wavelet filter bank branches can be simply understood by their frequency-masks. The planned scheme consists of two fragments. To obtain the low and high frequency coefficients simulation, a Matlab program can be used. at each decomposition scale, a reduction of a quarter in the scales of the 2-D circular-splitting regions can be achieved with he 2-D circular decomposition stage with down-sampling by (2, 2). The 2-D CSWT transform into (r + 1) low- and high-pass coefficients decompose the input noisy, where r is the number of the decomposition level. For the process of image de-noising, the decomposition stage of the 2-D CSWT can be adopted with some thresholding processes being applied on all high-pass coefficient channels. To maintain as much as possible noise-free high-pass channels, different thresholding levels can be applied. The 2-D circular-support reconstruction filter bank can result the de-noised image. In this stage, up-sampling by (2, 2) can be applied at each level to have the same size of the original image at the output.

4. Results

4.1 Conventional wavelet Results for Lena image with Gaussian noise

In this sub-section, the performance of the conventional wavelet de-noising by thresholding is evaluated by testing the same pre-mentioned Lena noisy test image. The same three pre-defined levels of Gaussian noise are used in that evaluation. The noisy Lena image with low-level Gaussian noise; variance = 0.001 & mean = 0 is shown in Figure 5 (a). The corresponding reconstructed Lena image using conventional wavelet de-noising by thresholding is shown in figure 5 (b) with Correlation = 0.98 and PSNR = 29.51 dB.

(a) (b)

Figure 5: (a) Noisy Lena image with low-level Gaussian noise; variance = 0.001 & mean = 0, (b) The corresponding reconstructed Lena image using conventional wavelet de-noising by thresholding; Correlation = 0.98 and PSNR = 29.51 dB.

The noisy Lena image with mid-level Gaussian noise; variance = 0.01 & mean = 0 is shown in figure 6 (a). The

corresponding reconstructed Lena image using conventional wavelet de-noising by thresholding is shown in figure 6 (b) with Correlation = 0.96 and PSNR = 25.12 dB.

The noisy Lena image with high-level Gaussian noise; variance = 0.1 & mean = 0 is shown in Figure 7 (a). The corresponding reconstructed Lena image using conventional wavelet de-noising by thresholding is shown in Figure 7 (b) with Correlation = 0.91 and PSNR = 21.04 dB.

(a) (b)

Figure 6: (a) Noisy Lena image with mid-level Gaussian noise; variance = 0.01 & mean = 0, (b) The corresponding reconstructed Lena image using conventional wavelet de-noising by thresholding; Correlation = 0.96 and PSNR = 25.12 dB.

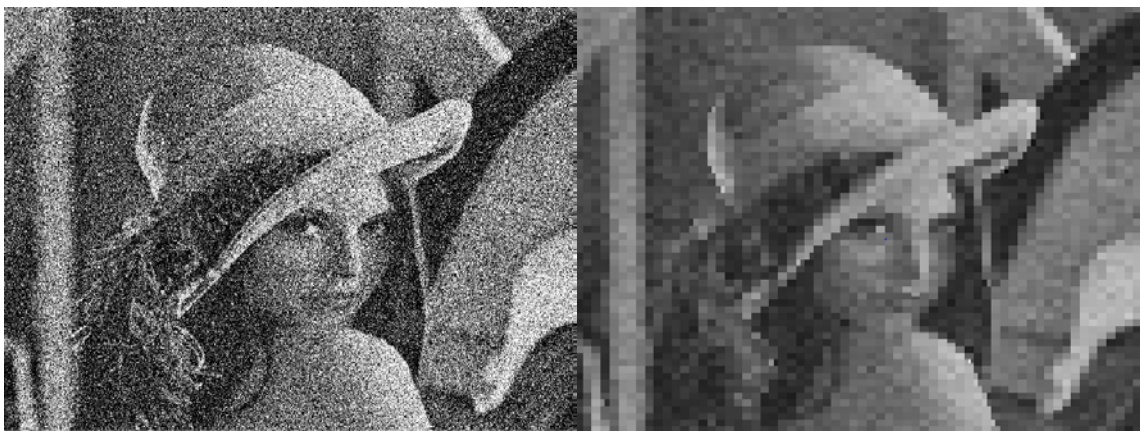

(a) (b)

Figure 7: (a) Noisy Lena image with high-level Gaussian noise; variance = 0.1 & mean = 0, (b) The corresponding reconstructed Lena image using conventional wavelet de-noising by thresholding; Correlation = 0.91 and PSNR = 21.04 dB.

4.2 Conventional wavelet Results for Lena image with salt and pepper Noise

It has been noted that conventional wavelet de-noising by thresholding cannot handle the salt and pepper noise So, the tests are cancelled.

4.3 Circular wavelet Results for Lena image with Gaussian noise

In this sub-section, the performance of the proposed circular wavelet de-noising scheme is evaluated via the above mentioned testing Lena noisy image.

Three levels of Gaussian noise are used in that evaluation.

These levels of Gaussian noise are low-level noise with variance = 0.001, mid-level noise with variance = 0.01 and high-level noise with variance = 0.1.

The noisy Lena image with low-level Gaussian noise; variance = 0.001 & mean = 0 is shown in Figure 8 (a). The corresponding reconstructed Lena image using circular wavelet de-noising scheme is shown in Figure 8 (b) with Correlation = 0.9921 and PSNR = 31.6530 dB.

(a) (b)

Figure 8: (a) Noisy Lena image with low-level Gaussian noise; variance = 0.001 & mean = 0, (b) The corresponding reconstructed Lena image using circular wavelet de-noising scheme; Correlation = 0.9921and PSNR = 31.6530 dB.

The noisy Lena image with mid-level Gaussian noise; variance = 0.01 & mean = 0 is shown in Figure 9 (a).

The corresponding reconstructed Lena image using circular wavelet de-noising scheme is shown in Figure 9 (b)

with Correlation = 0.9833 and PSNR = 28.3812 dB.

(a) (b)

Figure 9: (a) Noisy Lena image with mid-level Gaussian noise; variance = 0.01 & mean = 0, (b) The corresponding reconstructed Lena image using circular wavelet de-noising scheme; Correlation = 0.9833 and PSNR = 28.3812 dB.

The noisy Lena image with high-level Gaussian noise; variance = 0.1 & mean = 0 is shown in Figure 10 (a). The corresponding reconstructed Lena image using circular wavelet de-noising scheme is shown in Figure 10 (b) with Correlation = 0.9074 and PSNR = 20.4518 dB.

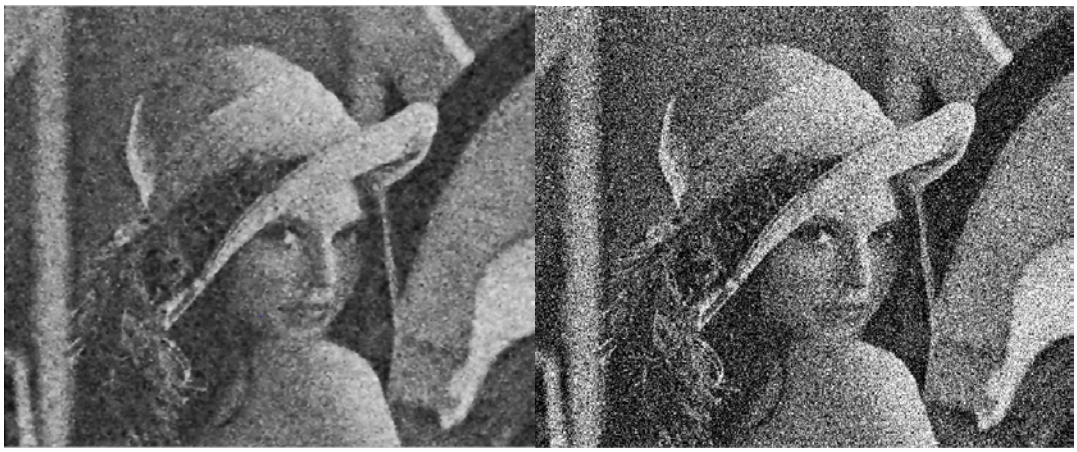

(a) (b)

Figure 10: (a) Noisy Lena image with high-level Gaussian noise; variance = 0.1 & mean = 0, (b) The corresponding reconstructed Lena image using circular wavelet de-noising scheme; Correlation = 0.9074 and PSNR = 20.4518 dB.

4.4 Circular wavelet results for Lena image with salt and pepper noise

In this sub-section, the performance of the proposed circular wavelet de-noising scheme is evaluated via the same pre-mentioned Lena testing noisy image. Three levels of salt and pepper noise densities are used in the evaluation. These levels of noise densities are low-level noise density of 0.001, mid-level noise density of 0.01 and high-level noise density of 0.1. The noisy Lena image with a low-level noise density of 0.001 (salt and pepper noise) is shown in Figure 11 (a). The corresponding reconstructed Lena image using circular wavelet de-noising scheme is shown in Figure 11 (b) with Correlation = 0.9932 and PSNR = 32.2770 dB.

(a) (b)

Figure 11: (a) Noisy Lena image with a low-level noise density of 0.001 (salt and pepper noise), (b) The corresponding reconstructed Lena image using circular wavelet de-noising scheme;
Correlation = 0.9932 and PSNR = 32.2770 dB.

The noisy Lena image with a mid-level noise density of 0.01 (salt and pepper noise) is shown in Figure 12 (a). The corresponding reconstructed Lena image using circular wavelet de-noising scheme is shown in Figure 12 (b) with Correlation = 0.9916 and PSNR = 31.3539 dB.

(a) (b)

Figure 12: (a) Noisy Lena image with a mid-level noise density of 0.01 (salt and pepper noise), (b) The corresponding reconstructed Lena image using circular wavelet de-noising scheme;
Correlation = 0.9916 and PSNR = 31.3539 dB.

The noisy Lena image with a high-level noise density of 0.1 (salt and pepper noise) is shown in Figure 13 (a). The corresponding reconstructed Lena image using circular wavelet de-noising scheme is shown in Figure 13 (b) with Correlation = 0.9733 and PSNR = 26.4267 dB.

(a) (b)

Figure 13: (a) Noisy Lena image with a high-level noise density of 0.1 (salt and pepper noise), (b) The corresponding reconstructed Lena image using circular wavelet de-noising scheme; Correlation = 0.9733 and PSNR = 26.4267 dB.

5. Conclusion

This paper has been presented and tested a new image de-noising scheme based on a 2-D CSWT. The performance of the proposed system has been examined by calculating metrics; such as PSNR correlation factors values of the resulting reconstructed de-noised image. A comparative study has been done between the conventional wavelet de-noising method and the proposed circular wavelet de-noising scheme. It has been noted that the 2-D CSWT can handle the salt and pepper noise while the conventional wavelet de-noising by thresholding cannot handle this type of noise.A better performance has been obtained from the proposed scheme as the Gaussian noise level is increased which means the proposed scheme is more suitable exactly for medium-level noise values (variance= 0.01) and generally for high-level noise values (variance= 0.1).

References

[1] B. Ergen, “Signal and Image Denoising Using Wavelet Transform”, Advances in Wavelet Theory and Their Applications in Engineering, Physics and Technology, A book edited under CC BY 3.0 license by Dumitru Baleanu, ISBN 978-953-51-0494-0, April 2012.

[2] C. Xiong, J. Tian, and J. Liu, “Efficient Architectures for Two-Dimensional Discrete Wavelet

Transform using Lifting Scheme", IEEE Transactions on Image Processing, Vol. 16, No. 3, pp. 607 – 614, March 2007.

[3] F. Vatansever, F. Uysal and A. Uzun, "Ayrik Dalgacik Dönüşümü İle Gürültü Süzme", 2007, www.emo.org.tr/ekler/7841cc9e552bd5c_ek.pdf.

[4] M. İkiz, M. Akin, B.Kurt and H. Acar, "Recognation The Speaker Identy By Means Of Wavelet Analysis And Neural Network", Doğu Anadolu Bölgesi Araştırmaları, 2007.

[5] B. Demir and S. Ertürk, "Wavelet Denoising Before Support Vector Classification of Hyperspectral Images", SIU 2007- IEEE 15th Conference on Signal Processing and Communications Applications, 1-13 June 2007, Eskisehir, Turkey, 2007.

[6] M. K. Singh, "Denoising of Natural Images Using the Wavelet Transform", M. Sc. Paper submitted to The Faculty of the Department of Electrical Engineering, San Jos´e State University, Dec. 2010.

[7] B. Ergen and M. Baykara, "Analysis of De-noising with Wavelet and Wavelet Package Decomposition", E-Journal of New World Sciences Academy, Vol. 6, No. 2, pp. 518-526, 2011.

[8] M. Üstündağ, E. Avci, M. Gökbulut and Fikret Ata, "Denoising of Weak Radar Signals using Wavelet Packet Transform and Genetic Algorithm", Journal of the Faculty of Engineering and Architecture of Gazi University, Vol. 29, No. 2, pp. 375-383, 2014.

[9] A. Srivastava and S. Maheshwari, "Signal Denoising and Multiresolution Analysis by Discrete Wavelet Transform", Innovative Trends in Applied Physical, Chemical, Mathematical Sciences and Emerging Energy Technology for Sustainable Development, 2015. www.krishisa nskriti.org/vol_image/23Sep201506092619.pdf.

[10] M. Mastriani, "Quantum Boolean image denoising", Quantum Inf. Process, Vol. 14, pp. 1647–1673, 2015.

[11] J. M. Abdul-Jabbar, Z. T. Abede and A. A. Dawood, "A Multiplier-less Implementation of Two-Dimensional Circular-Support Wavelet Transform on FPGA", Iraq J. Electrical and Electronic Engineering, Vol.9, No.1, pp. 16-28, 2013.

[12] J. M. Abdul-Jabbar and Z. N. Abdulkader, " Iris Recognition using 2-D Elliptical–Support Wavelet Filter Bank", International Conference on Image Processing Theory, Tool and Applications- IPTA 2012, Istanbul, Turkey, 15-18 Oct., pp. 359 – 363, 2012.

[13] J. M. Abdul-Jabbar and H. N. Fathee, "Design and Realization of Circular Contourlet Transform", Al-Rafidain Engineering Journal, Vol. 18, No. 4, pp. 28 - 42, Aug. 2010.